Astron. Astrophys. 256, 463–476 (1992)

ASTRONOMY AND ASTROPHYSICS

A photometric survey of the eclipsing RS CVn-type system RZ Eridani: starspot variability, circumstellar matter, tidal evolution*

G. Burki[1], **Z. Kvíz**[2,1], **and P. North**[3]

[1] Observatoire de Genève, CH–1290 Sauverny, Suisse
[2] School of Physics, University of New South Wales, Kensington NSW 2033, Australia
[3] Institut d'Astronomie, Université de Lausanne, CH–1290 Chavannes-des-Bois, Suisse

Received August 29, accepted December 2, 1991

Abstract. The RS CVn-type eclipsing binary RZ Eridani has been monitored in the 7 colours of the Geneva photometric system between November 1977 and April 1989. It is shown that the primary is an A8-F0IV star and has been stable during the survey. The distortion of the light curve between eclipses, the migration wave, is entirely due to the variability of the secondary component, a G8-K0IV-III star. This variability is characterized by:

- a starspot effect varying from year to year, with a period of about 35 d , related to the stellar rotation period;
- a reflection effect of the light of the primary component, with a period equal to the orbital one;
- a long-term effect which could be due to a stellar activity cycle.

The light curve has been corrected for the secondary component variability and analysed with the program EBOP (Etzel, 1980). The existence of the secondary eclipse at phase 0.67 is confirmed and the following parameters are derived, by using in addition the results of Popper (1988) from the radial velocity curves of both components:

orbit	:	P	=	$39^d.28254$
		T_o	=	2446048.883
		e	=	0.377
		ω	=	$-47°.3$
		i	=	$89°.30$
radii	:	R_A	=	$2.79 \pm 0.12 R_\odot$ (hotter star) and
		R_B	=	$6.80 \pm 0.23 R_\odot$ (cooler star)
masses:	:	M_A	=	$1.69 \pm 0.06 M_\odot$ and
		M_B	=	$1.63 \pm 0.13 M_\odot$

The effective temperatures, luminosities and age are also determined. The light from RZ Eri is affected by a rather strong reddening, E(B-V) = 0.20 for d = 180pc and b = −33°, probably mostly due to circumstellar material.

The spectral types of both components and the amount of reddening are confirmed by the analysis of UV low resolution spectra obtained from the IUE satellite database. It is shown that the extinction law for this circumstellar matter is similar to the standard interstellar extinction law.

The orbit of RZ Eri is not yet circularized, but this ought to occur when the cooler component which is now at the bottom of the red giant branch, will have evolved past the tip of this branch, because its radius will reach there a maximum value of more than 30 $R_\odot$.

The hotter component, located at the end of the main-sequence stage, rotates faster ($P_{rot} \sim 2^d.5$) than the pseudosynchronisation period of RZ Eri $P_{ps} = 20^d.4$, while the cooler component rotates slower ($P_{rot} \sim 34$d) than P_{ps}. This is a consequence of the difference in the evolutionary stages of both components, RZ Eri B having experienced a rapid expansion of its radius during its recent crossing of the Hertzsprung gap.

Key words: stars: RZ Eridani – stars: binaries: general – stars: variable, stars:rotation of – stars: circumstellar matter – photometry

1. Introduction

RZ Eri (HD 30050) is a relatively bright ($m_V = 7^m.7$) eclipsing system with a deep primary minimum ($1^m.1$ in m_V) and newly detected secondary. With its orbital period of 39.28 days, it is a member of the long period group of the RS Canum Venaticorum binaries (Hall, 1976). Originally, they were systems with periods varying between one day and two weeks, spectral class F or G for the hotter component and which display strong H and K CaII emission outside eclipse. This classification has further been extended to include systems having longer or shorter periods.

Feckel et al. (1986) discussed the definition of the various groups of active stars and they proposed the following characteristics for the RS CVn-type group:

i) at least one star has strong CaII H and K emission.
ii) the system has periodic light variations not caused by pulsation, eclipses, ellipticity.
iii) the more active star is an F, G or K subgiant or giant. There is no restriction on the spectral type of the other star and on the orbital period.

The general properties of RS CVn-type systems have been reviewed by Montesinos et al. (1988). In particular, they show that the evolutionary status of these binary stars is not completely understood. They note that RZ Eri and some other systems had an

Send offprint requests to: G. Burki
*Based on observations made at the European Southern Observatory, La Silla, Chile

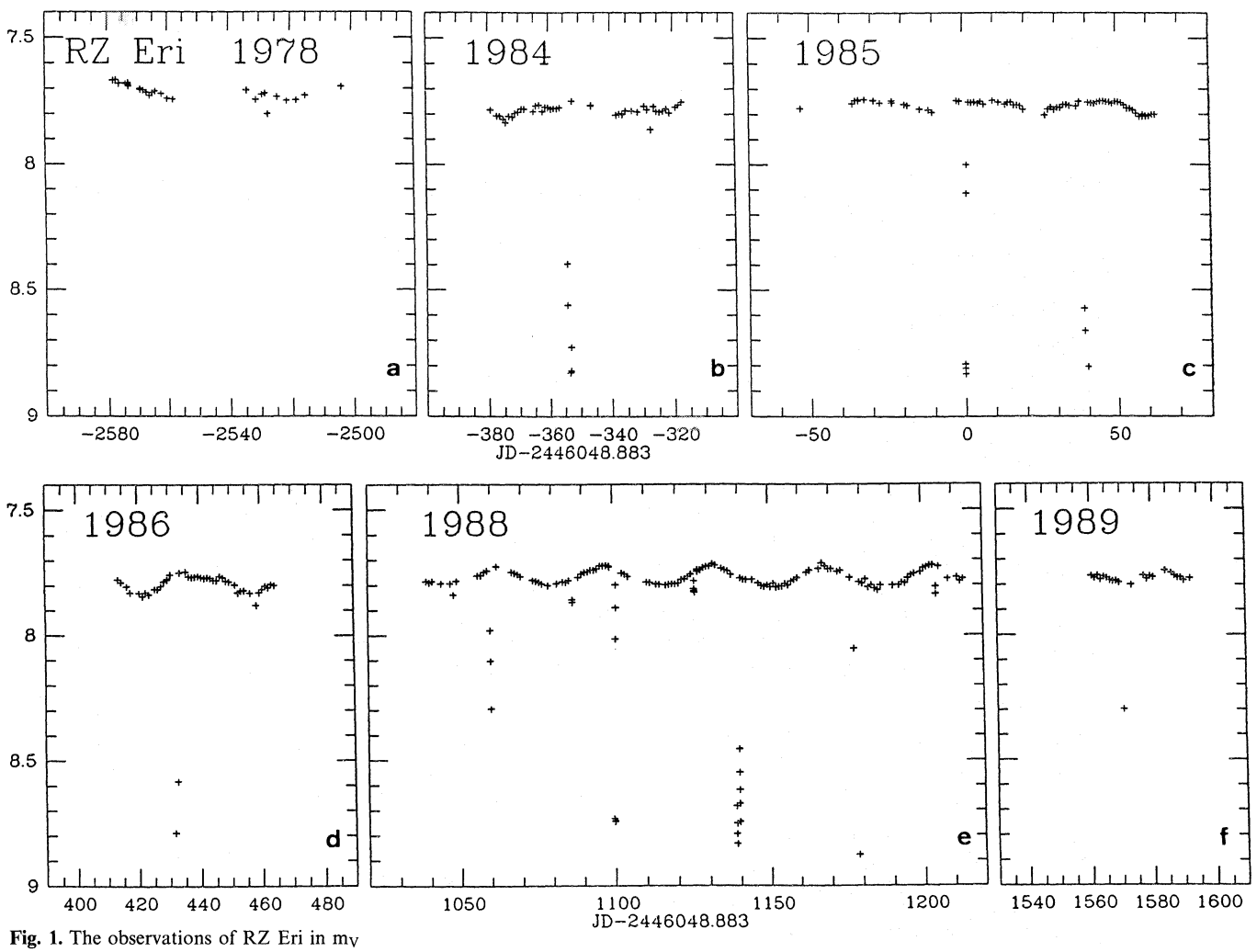

Fig. 1. The observations of RZ Eri in m_V

abnormal evolution, i.e. the more massive star is the less evolved or the components with similar masses show a large difference between the radii. The evolutionary scenario of Popper & Ulrich (1977) can explain the configuration of these systems, if the rapid crossing of the Hertzsprung gap by the first evolving component is characterized by a mild mass exchange ($\lesssim 5 \cdot 10^{-11} M_\odot y^{-1}$) and mass loss. In this context, it must be noted that, with the values of the masses with their uncertainties as determined in Sect. 6 of the present paper, it is quite possible that the most evolved component of RZ Eri is in reality also the most massive, by at most about one tenth of $M_\odot$.

One of the characteristics, common to many of the RS CVn-type systems, is a distortion of the light curve which migrates in phase with respect to the eclipses. The most accepted theory for the explanation of the distortion wave is the starspot model, i.e. the surface of the differentially rotating star exhibits dark and/or bright spots changing in size and brightness with time.

So far, the best light curve solution and radial velocity curve interpretation for RZ Eri has been obtained by Popper (1988) who gave masses and radii of $1.68 \pm 0.10 M_\odot$ and $2.83 \pm 0.24 R_\odot$ for the hotter component, and $1.62 \pm 0.20 M_\odot$ and $7.0 \pm 0.3 R_\odot$ for the cooler one. Spectral classification causes problems because the colours of both components seem to be anomalous according to Popper, who derived the types F5V and K2III-K5V. Another classification, by Sarma (1986), gives the types F6V and K2IV. Our photometric classification established earlier spectral types for both components (see Appendix).

According to the radial velocity curve obtained by Cesco & Sahade (1945), the orbit of RZ Eri has a high eccentricity of 0.37. This fact was confirmed by Popper (1988) and Imbert (1991), who derived respectively 0.35 and 0.37 on the basis of their radial velocity analyses. The suspicion of the existence of a secondary minimum in the light curve at phase 0.67, in agreement to the above value of the eccentricity, was mentioned by Caton (1986) and is completely confirmed in the present study.

The distortion of the light curve outside eclipses was analyzed by Caton (1986) who suggests a wave of a few hundredth of a magnitude in total amplitude. The variability was confirmed by the survey of Strassmeier et al. (1989), showing a light curve shape similar to our observations.

RZ Eri has been monitored in the Geneva seven colour photometric system (Golay, 1980; Rufener, 1988) from the Swiss station at the ESO La Silla Observatory in Chile. A total of 383 photometric measurements were recorded between November 22, 1977 and April 24, 1989. The entire set of data was obtained with the same two-channel aperture photometer (Burnet & Rufener,

1979), the same set of 7 passbands (Rufener & Nicolet, 1988) and the reductions were carried out according to the procedures defined by Rufener (1964, 1985). Two telescopes have been used, a 40 cm before 1980 and a 70 cm later on. Preliminary results based on this survey of RZ Eri have been published by Kvíz (1989) and Burki (1991).

2. The observations

The Geneva photometric data of RZ Eri are listed in Table 1 [1]. Recall that the Geneva indices [U-B] and [B-V] are not normalized to zero for an A0 V star as it is the case for the Johnson UBV indices.

The magnitudes in each of the 7 Geneva filters are obtained from m_V and the 6 colour indices in the following manner:

$$m_i = m_V - [V-B] + [i-B] \quad (1)$$

with i representing one of the 7 filters U, B, V, B1, B2, V1, G.

Figures 1a to 1f show the variability of RZ Eri in V magnitude from year to year. We clearly see:

1. The primary eclipse, observed partially nine times. The magnitude at the light minimum is about $m_V = 8.9$.
2. The variation outside eclipses. Especially noteworthy is the regular "migration wave" observed betwen October 1987 and April 1988 (HJD-T_o between 1039 and 1214, see Fig. 1e).
3. The secondary eclipse, observed in 6 cases, for HJD-T_o = −327, 459, 1048, 1087, 1126, 1205. Fig. 2 shows the "global" light curve obtained by plotting all the observed points versus the phase calculated by using the above values for P and T_o. Despite the large scatter due to the migration wave (variability of the secondary component, see Sect. 4), the **secondary eclipse** is clearly visible at phase 0.67. Recall that the presence of a secondary eclipse at this phase was suspected by Caton (1986).

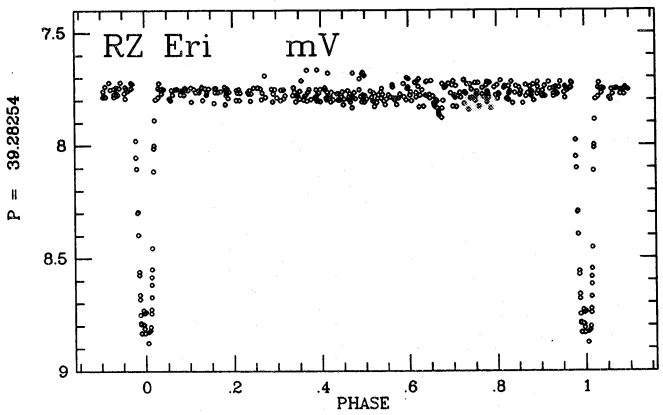

Fig. 2. The global light curve or RZ Eri. Noteworthy are the secondary eclipses at phase 0.67 and the large scatter due to the variability of RZ Eri B

The values of the orbital period and epoch of the primary eclipse used in this paper are:

P = $39.28254 \pm 0^d.00005$
T_o = 2'446'048.883 [HJD]

[1]Table 1 is available on request to the authors.

They have been determined by using O-C technique in a similar way as Hall & Kreiner (1980) but with a larger number of points, and by varying the value of P in our EBOP solution (see Sect. 6) in order to have the lowest residuals. We also conclude that the period did not vary since the beginning of the century.

3. The primary component

Figure 3 shows the global light curve during the primary eclipse. Since this eclipse is total, the scatter in the phase interval 0.989-1.011 can be attributed to the secondary component only.

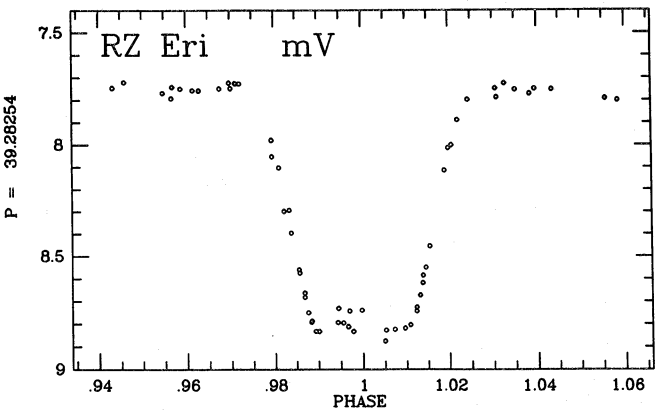

Fig. 3. The global light curve during the primary eclipse

Table 2. The seven Geneva magnitudes of RZ Eri A, determined during 7 primary eclipses.

	mag.	observed s.d.	expected s.d.
m_V	8.269	0.011	0.011
m_U	9.618	0.007	0.009
m_B	7.878	0.010	0.008
m_{B1}	8.894	0.012	0.008
m_{B2}	9.241	0.014	0.010
m_{V1}	9.009	0.013	0.011
m_G	9.354	0.017	0.013

It is possible to calculate the magnitude of the primary component, at the epoch of each individual eclipse, by substracting the flux of the secondary (bottom of the eclipse) from the flux of both components (just before and after the eclipse). This calculation has been made for each of the seven Geneva magnitudes and for each of the seven primary eclipses for which data have been recorded during the phase of totality. The results are given in Table 2.

The observed standard deviations come from the data on the seven eclipses, and the expected standard deviation is given by

$$\sigma^2_{m_A} = \left(\frac{F_{A+B}}{F_A}\right)^2 \sigma^2_{m_{A+B}} + \left(\frac{F_B}{F_A}\right)^2 \sigma^2_{m_B} \quad (2)$$

where F_A, F_B, F_{A+B} are the primary, secondary and total (outside eclipse) fluxes. The uncertainties $\sigma_{m_{A+B}}$ and σ_{m_B} are derived from

the mean σ_{m_V} vs. m_V relation obtained for the well-measured southern field stars in the Geneva catalogue (Rufener 1988, Fig. 2). The observed and expected standard deviations are of comparable magnitudes. Thus, the conclusion is that **the primary component of RZ Eri has not varied during our survey**.

In the Appendix are presented the results of our photometric analysis of both components of RZ Eri . On the basis of our data in Geneva photometry and of the study of some UV spectra from the IUE satellite (see Sect. 5), it is shown that the primary component has the following characteristics:

Spectral type	:	A8-F0IV
Absolute magnitude	:	$M_V = 1^m.41 \pm 0.15$
Distance	:	180pc
Visual extinction	:	$A_V = 0^m.65$

It is shown in Sect. 5 that the visual extinction is mostly **circumstellar**. As shown in the Appendix, the high value of the total (i.e. circumstellar and interstellar) visual extinction is probably the cause of the discordant colour indices noted by Popper (1988) who adopted a negligible reddening on the basis of the value of the galactic latitude (−33°).

4. The secondary component

The stability of the primary component implies that the variability outside eclipses of RZ Eri is completely due to the secondary component. After substraction of the primary flux (from Table 2) from the total flux (from Table 1), it is possible to analyse the variability of the secondary component alone.

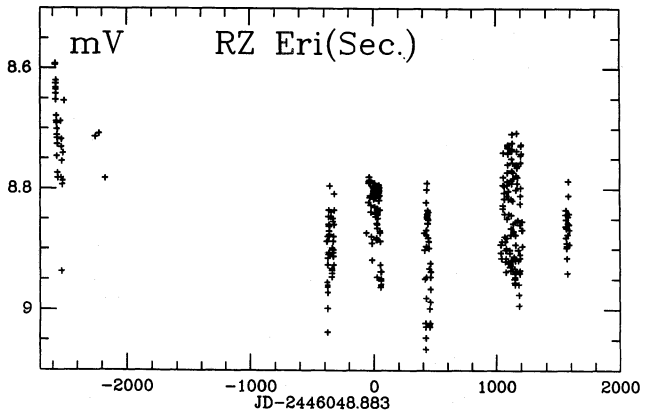

Fig. 4. The m_V magnitude of RZ Eri B outside eclipses

In Fig. 4, a very long-term variability is clearly visible. In particular, the V magnitude became fainter by about $0^m.2$ from 1978 to 1984. This kind of variability can be tentatively attributed to a **stellar activity cycle**.

The mean 7 Geneva magnitudes of the secondary component have been calculated (see Table 3). These values are important in order to analyse the colours of the star. Because of the long-term variability described above, only the measurements for HJD > 2 445 600 have been taken into account. Note that the effect of this variability on the colour indices is negligible, thus the photometric classification obtained in the Appendix is not affected by this change in the magnitudes. It is shown that the secondary component has the following characteristics:

Spectral type	:	G8-K2IV-III
Absolute magnitude	:	$M_V = 1.85 \pm 0.17$

Table 3. The seven mean Geneva magnitudes of RZ Eri B. Only the measurements outside the eclipses and later than HJD 2 445 600 have been used.

magnitudes						
m_V	m_U	m_B	m_{B1}	m_{B2}	m_{V1}	m_G
8.863	11.214	9.289	10.564	10.452	9.632	9.762

As described in Sect. 2, a short-term variability, the migration wave, is present in each set of data. As already said, this is due to the variability of the secondary. A particularly good series of measurements was obtained from October 18, 1987 to April 1, 1988.

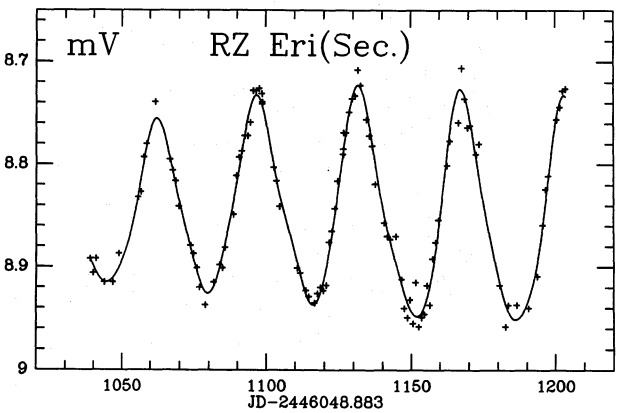

Fig. 5. The light curve of RZ Eri B outside eclipses between October 18, 1987 and April 1, 1988

Figure 5 shows this exceptionally regular light curve. The fitted curve is a Fourier fit with 3 components:

a) A large amplitude **starspot effect**: the peak-to-peak amplitude is $0^m.185$, the light curve is slightly asymmetric and the period of $34^d.903$ corresponds to the mean rotational period of the spots on the stellar surface. This component is shown in Fig. 6a.

b) A variability of period $39^d.283$, equal to the orbital period, and amplitude $0^m.044$ (see Fig. 6b). The phase of the light maximum is 0.67, corresponding exactly to the secondary eclipse. Thus, this component can be identified as the **reflection effect** of the light of the primary component on the atmosphere of the secondary component. However, the observed amplitude seems too large with respect to the predictions of the programs EBOP (Etzel, 1980) or WINK (Wood, 1971, 1972) used to analyse the light curve of eclipsing systems (see section 6). From the amplitude of $0^m.044$ on the secondary component, a variation of 1.8% on the total luminosity of the system is obtained. The modelling of this effect by WINK predicts a variation of 0.4% only, by using an albedo of 0.4 for the secondary component corresponding to the convective case (Rucinski, 1969, Söderhjelm, 1980). Thus, the "observed" value for the reflection effect is roughly 4 times larger than the predicted value. The possible explanations for this discrepancy are:

i) the observed effect is overestimated due to the whitening procedure in the Fourier analysis (the starspot effect is 4.2

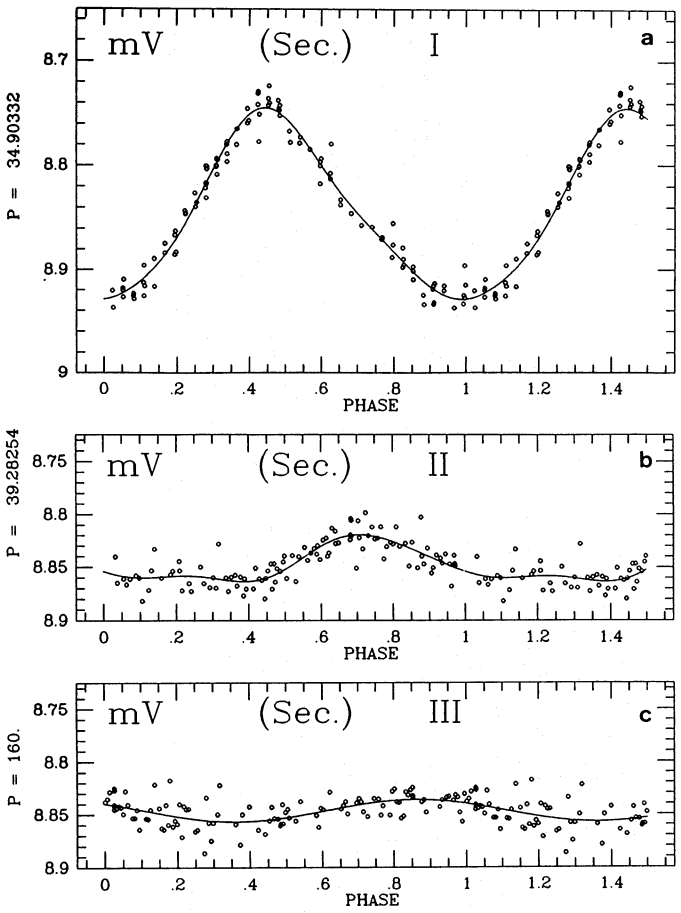

Fig. 6. The three components of the light curve of RZ Eri B: I starspot effects, II reflection effect, III activity cycle (?)

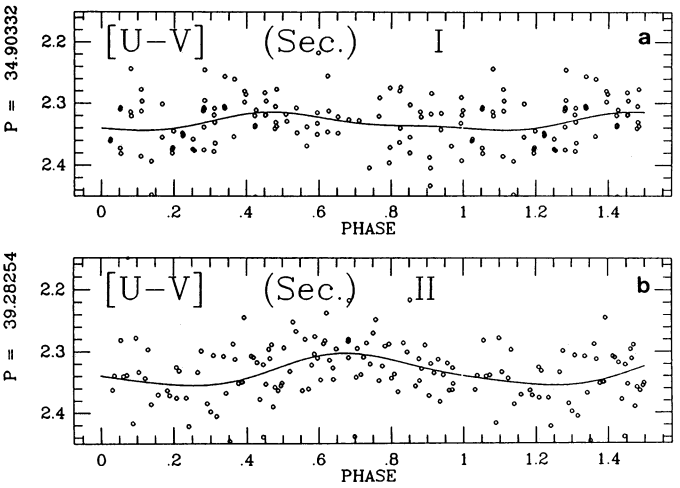

Fig. 7. Same as Fig. 6 but for the colour index [U-V]

Table 4. The main characteristics of the light curve of RZ Eri B during 4 seasons of observation.

	1984	1985	1986	1988
Period	$34^d.556$	36.252	35.919	34.903
mean mag. $<m_V>$	8.882	8.844	8.904	8.846
m_V max	8.768	8.795	8.792	8.745
m_V min	8.973	8.956	9.060	8.928
peak-to-peak amplitude	0.205	0.161	0.268	0.183

times larger, and its period and amplitude are certainly not strictly constant during 175 days);

ii) another effect induces a light variation with a period equal to P_{orb}, as for example an inhomogeneous distribution of the circumstellar matter (see section 5) or a diffusion of the light from the components by this matter.

c) A mid-term variability of period ~ 160d and peak-to-peak amplitude $0^m.02$. This period is very imprecise since its value corresponds to the time interval of the observations. This variability could be connected to the **activity cycle** (see Fig. 6c).

The residual standard deviation of the observed points around the 3 components fitted curve is $0^m.011$, a quite satisfying value taking into account that the starspot variability normaly changes from cycle to cycle and that we observed 4.5 rotation cycles during the season 1987–1988. As shown in Fig. 7, both starspot and reflection effects produce colour variations. In [U-V] colour the peak-to-peak amplitudes are $0^m.029$ for the starspot variation and $0^m.052$ for the reflection effect. The corresponding amplitude ratios in [U-V] and m_V are respectively 0.16 and 1.2. For these both effects, the star is bluer when brighter. On the other hand, the dispersion is much higher in the colour [U-V] curve than in magnitude m_V curve: respectively $0^m.041$ and $0^m.011$.

The shape and the period of the light curve due to the spots vary from year to year (and even from one cycle to another), due to the migration of the spots and to their changes in size and brigthness. This is visualized in Fig. 8, showing the light curve of the secondary component during 4 seasons of the survey. The reflection effect, as determined for the year 1988 (Fig. 6b), has been substracted from the data and, for each year, the best period has been determined and a fit of Fourier series with 2 harmonics in addition to the fundamental frequency has been performed. The best values of the period are: $34^d.556$ in 1984, $36^d.252$ in 1985, $35^d.919$ in 1986 and $34^d.903$ in 1988. These 4 light curves due to the starspots are shown together in Fig. 9 where they are plotted with respect to the phase (the period changes). Displacements in phase have been applied in order to have, in each case, the light minimum at phase zero.

The values of the mean, maximum and minimum magnitudes are given for each year in Table 4.

The main characteristics of the light curve variation are the following:

1. The value of the luminosity maximum changes significantly less than the value of the luminosity minimum: respectively $0^m.047$ and $0^m.132$ in the case of these 4 seasons of observation.
2. The "system" of the starspots on the stellar surface was the simplest in 1985: the plateau at maximum light between phases 0.4 and 0.7 could indicate that the spot(s) has an extension of about 70° in stellar longitude, corresponding to 0.20 in phase through the stellar rotation.
3. The system of the spots was more complex in 1984: at least 3 or 4 spots seem necessary to explain the shape of the light curve.

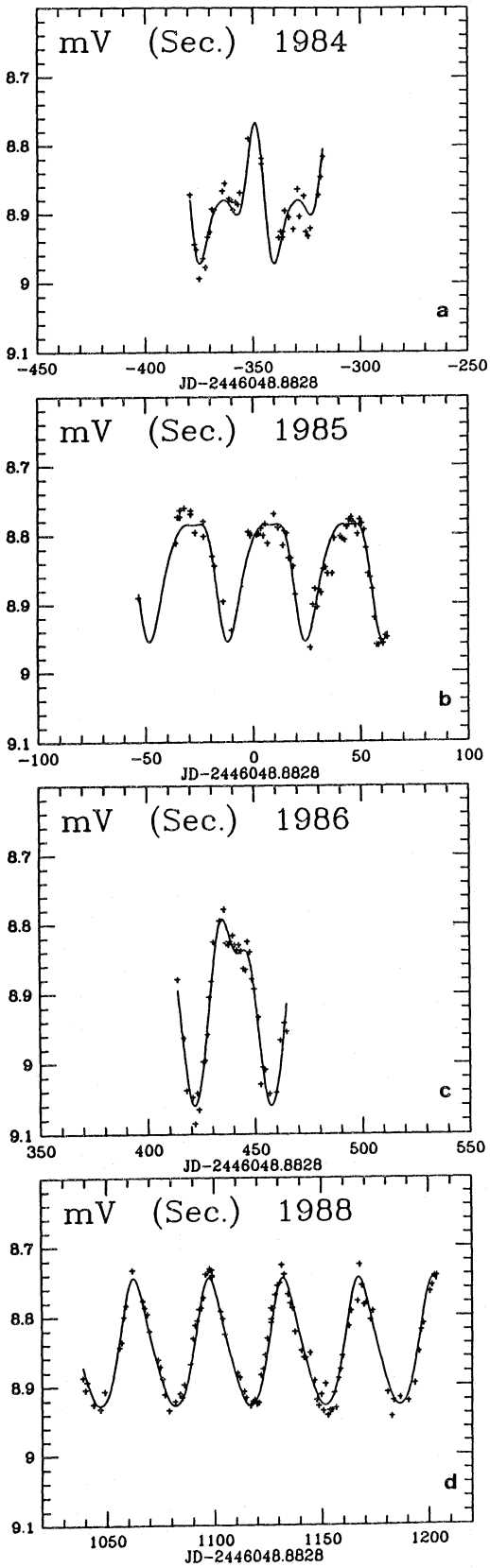

Fig. 8. The light curves due to the starspot effects during 4 seasons of observations

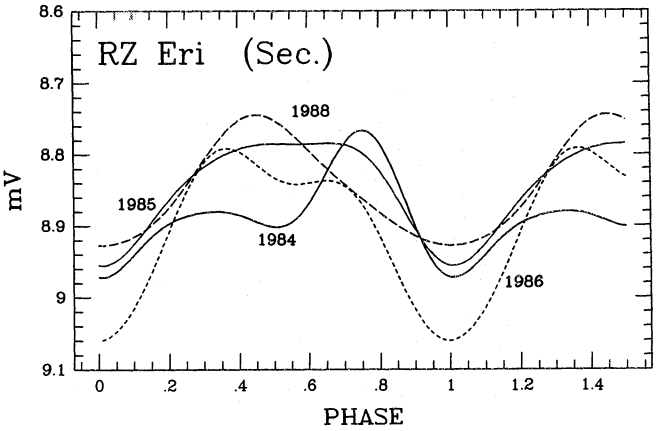

Fig. 9. Variation of the light curve due to the starspot effect

4. In 1988, the light curve has a nearly sinusoidal shape. It could be explained by a very large spot expanding over the whole surface in stellar longitude but having a continuously variable extension in latitude.

In complement to this qualitative description of the light curve, it must be emphasized that a detailed analysis in terms of brightness inhomogeneities of the stellar surface requires a spectral imaging reconstruction applied to variable profile of chromospheric lines, as the CaII line (e.g. Rodono, 1986).

Finally, the period of the starspot variability is related to the rotation of the secondary component, which is supposed to be differential. In consequence, the equatorial rotational period of the secondary must be smaller or equal to the smallest observed starspot period, i.e. $P_{eq}(rot) \leq 34^d.5$.

5. The circumstellar matter

The total visual extinction towards RZ Eri derived in the Appendix is very high, $A_V = 0^m.65$, with respect to the distance, 180 pc, and galactic latitude, $b = -33°$. The visual inspection of the Palomar photographic plate does not reveal any evidence for an important amount of interstellar matter in this region of the Galaxy. This is confirmed by the study of Lucke (1978) on the distribution of interstellar reddening material in the solar neighbourhood.

5.1. Geneva photometry

In order to estimate the value of the extinction in the direction of RZ Eri, the Geneva photometric catalogue has been searched for an early-type star in the vicinity of RZ Eri. The calibrations of Cramer and Maeder (1979) and Cramer (1982), based on the Geneva reddening-free parameters X and Y (valid for B-type stars), have been applied to HD 30332, a (B9)-type star located at an angular distance of 64′ from RZ Eri. The following values are derived: spectral type B9III, $M_V = -0.5$, $E(B_2\text{-}V_1) = 0^m.053$, distance of 390pc, total visual extinction $A_V = 0^m.19$. This value of A_V is only 29% of that of RZ Eri while its distance is twice larger.

In consequence, the essential part of the reddening towards RZ Eri ought to be attributed to **circumstellar matter**. By adopting the mean value of 0.49 mag/kpc, derived from HD 30332, to describe the mean interstellar extinction in this direction of the

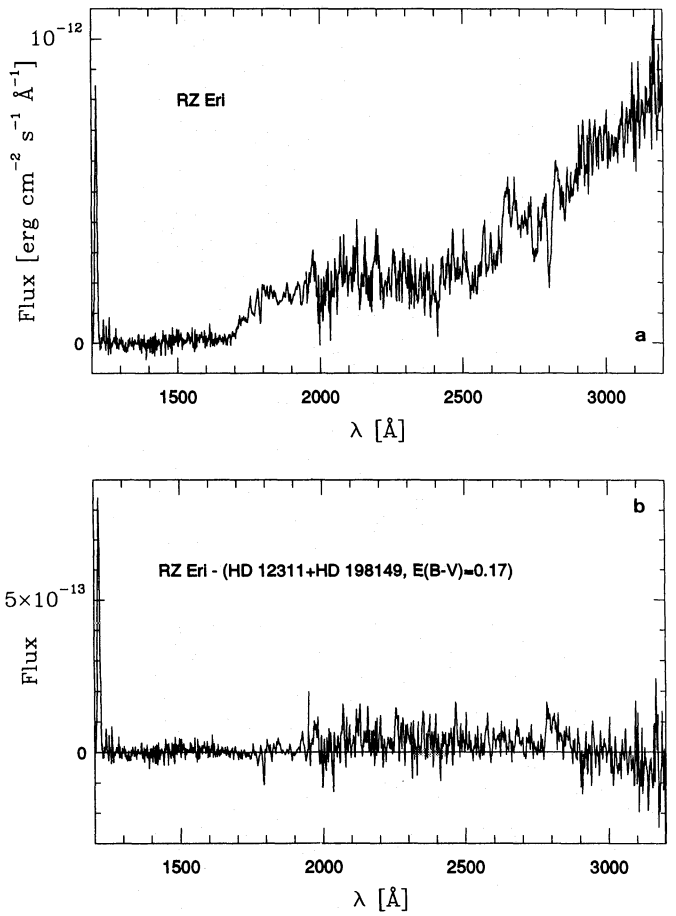

Fig. 10. a) IUE low resolution spectra of RZ Eri. **b)** Difference of the UV fluxes between RZ Eri and the addition of HD 12311 (simulating RZ Eri A) and HD 198149 (simulating RZ Eri B), attenuated by a circumstellar extinction characterized by E(B-V) = 0.17

Galaxy, it is found that the circumstellar visual extinction is $A_V = 0^m.56$ for RZ Eri.

5.2. *Ultraviolet with IUE*

It is interesting to test in the UV domain these conclusions obtained on the basis of optical photometric data, in particular the effective temperature (or spectral type) of the primary component and the amount of interstellar and circumstellar reddenings. The extinction being very high in the UV, it may also be possible to detect a possible deviation from the mean interstellar extinction law.

Fortunately, some low resolution UV spectra of RZ Eri are available in the USSP/ULDA database of the IUE satellite (Murray et al., 1990).

Table 5 gives the characteristics of the best exposed among these few spectra, in both short (SWP) and long (LWR) wavelength ranges of IUE. The orbital phases according to the ephemerides given in Sect. 2 are also given: these spectra have been taken $4^d.3$ before the beginning (LWR) and $2^d.6$ after the end (SWP) of the primary eclipse. Both spectra are presented together in Fig. 10a, with a joining at 2000 Å. The difference of signal-to-noise ratio between the two spectra is clearly visible.

We tried to reproduce the UV energy distribution of RZ Eri by adding the UV spectra of 2 typical stars having spectral types similar to those of both components as determined in the Appendix. This simulation work was made possible by the existence of the IUE database, with the help of the atlases of IUE spectra (Wu et al. 1983; Heck et al. 1984) and by using ESO's MIDAS software package (see the MIDAS User's Guide, distributed by the Image Processing Group, European Southern Observatory). The steps of this simulation are the following:

1. A trying value of the colour excess E(B-V) is chosen.
2. The unreddened apparent visual magnitudes m_A° and m_B° of both components of RZ Eri are calculated.
3. Two bright unreddened stars S_1 and S_2 are selected in the IUE database. Their spectral types must be similar to those of the components of RZ Eri. They have the visual apparent magnitudes m_1° and m_2°.
4. The apparent magnitude differences $m_A^\circ - m_1^\circ = 5 \log \frac{d_A}{d_1} = F_1$ and $m_B^\circ - m_2^\circ = F_2$ are calculated, with the hypothesis that $M_A^\circ = M_1^\circ$ and $M_B^\circ = M_2^\circ$.
5. The IUE fluxes of stars S_1 and S_2 are scaled according to the factors F_1 and F_2.
6. The two scaled UV fluxes are added and attenuated following the interstellar extinction law of Seaton (1979), and by adopting the same value of E(B-V) as that chosen in point 1.
7. This simulated UV flux is compared to the observed one of RZ Eri, i.e. the flux difference observed–simulated is calculated. This difference depends on the choices of star S_1, star S_2, E(B-V). Of course, the result of this simulation is satisfactory if the flux difference is zero over the whole UV range.

A favourable result was obtained for the combination HD 12311 (F0V), HD 198149 (K0IV) and E(B-V) = 0.17, as shown in Fig. 10b (the IUE spectra of these two stars are referenced in Table 5). The flux difference is not perfectly equal to zero through the whole wavelength range, but we think it would not make sense to push the analysis further, because of the modest S/N ratio of the spectra of RZ Eri. The conclusions of this simulation are the following:

i) It is possible to find a combination of star S_1, star S_2, E(B-V) such as: 1. both stars have spectral types similar to those of the components of RZ Eri; 2. the colour excess is nearly identical to the value deduced from the optical analysis.

ii) The very small value E(B-V) = 0.03 obtained by Dobias & Plavec (1989) for RZ Eri is excluded by our analysis.

iii) An exotic extinction law is clearly not needed to reproduce the observed UV flux. Thus, the circumstellar matter in the vicinity of RZ Eri ought to have physical characteristics on the average similar to those of the interstellar material.

5.3. *IR excess*

The infrared emission of RS CVn-type binaries has been studied by Busso et al. (1990, and references given therein). They have fitted the IR observations by combinations of known stellar energy distributions of stars of various spectral types. In 40% of the 30 cases, an IR excess emerges, i.e. no combination of the IR energy distributions, simulating the primary and secondary components, can reproduce satisfactorily the observed IR flux of the system, an additional IR flux from circumstellar material must be taken into account.

RZ Eri is one of these systems, the best solution of Busso et al. (1990) having been obtained with stars of types A7IV-V and

Table 5. IUE images of RZ Eri and of the stars used in the selected simulation.

star	V	E(B- V)	Image N° & aperture	exp. time (s)	civil date & JD-2440000	orbital phase
RZ Eri	8.269 (prim) 8.863 (sec.)	0.17	SWP 15744L	900	14 Dec. 1981 4952.758	0.096
			LWR 11571L	360	17 Sept. 1981 4864.977	0.862
HD 198149 (KO IV)	3.426	0.00	LWR 12739L[a]	90	8 March 1982 5037.092	
HD 12311 (FO V)	2.852	0.00	SWP 11242L	37	5 Feb. 1981 4641.450	
			LWR 9862L	8.4	5 Feb. 1981 4641.443	

a: no SWP image exists, since the flux of this star is negligible in IUE's short wavelength range.

K3IV, and with an additional IR flux. Of course, the detection of this IR excess is a confirmation of a circumstellar shell or envelope around RZ Eri.

5.4. Origin of the circumstellar matter

According to the scenario by Popper and Ulrich (1977), a mild mass exchange accompanied by a mass loss ($\leq 5 \cdot 10^{-11} M_\odot y^{-1}$) during the crossing of the Hertzsprung gap by the first evolving component is necessary to account for the observed properties of the RS CVn-type systems. The detection of circumstellar matter around RZ Eri , together with the evolutionary status of its components (see Sect. 7), is in qualitative agreement with this scenario.

A circumstellar envelope has also been detected by Glebocki et al. (1986) around λ And, another long-period RS CVn-type system. This detection, based on the detailed analysis of MgII lines, is important for the present analysis, because λ And has characteristics similar to those of RZ Eri, in particular the long orbital and rotation periods, respectively $20^d.52$ and $53^d.95$. Moreover, the determination of P_{rot} was based on starspot photometric variations very similar to those of RZ Eri (Scaltriti et al., 1984).

In Sect. 7, the evolution of RZ Eri will be studied on the basis of the stellar evolutionary tracks by Maeder & Meynet (1988) for which the parametrisation of the mass loss rate by de Jager et al. (1988) has been used. According to these calculations, the mass loss rate for RZ Eri is presently $1.7 \cdot 10^{-11} M_\odot y^{-1}$, the total mass lost having been about $2 \cdot 10^{-4} M_\odot$ during the past $8 \cdot 10^6$y. This matter has been partially captured by the hot companion RZ Eri A, the rest having escaped out of the system. It is from this matter that circumstellar grains are supposed to be formed. Is this amount of mass lost by RZ Eri B compatible with the observed extinction by interstellar matter ?

The circumstellar part of the colour excess is estimated to E(B-V) = 0.17 (see Sect. 5.1.). For the following calculation, we make the hypothesis that the extinction law for this circumstellar matter is similar to the standard law of the interstellar matter in the Galaxy and that the ratio between the gas and dust densities is of the order of 100 (e.g. Martin, 1978). Note that this hypothesis seems justified by the results of Sect. 5.2. It is possible to estimate the column density of the gas surrounding RZ Eri by using the relation of Bohlin et al. (1978).

$$N(H) \cong 5.8 \cdot 10^{21} E\,(B-V) \text{ atoms cm}^{-2}$$

By supposing that this matter is isotropically distributed around the stars in a sphere of radius r, the total mass M of circumstellar matter in this volume is:

$$M \cong 1.4 \cdot 10^{-8} E\,(B-V) r^2 \qquad M(M_\odot), r\,(U.A.)$$

It results that $M \cong 2.4 \cdot 10^{-7} M_\odot$ if $r = 10$ U.A. and $M \cong 2 \cdot 10^{-4} M_\odot$ if $r = 300$ U.A.. In addition, the envelope of circumstellar matter can be non-spherical. The so-called common envelope phase in the evolution of a binary system can be characterized, in some circumstances, by a mass ejection taking place in a narrow region around the equatorial plane, with a half-angle of rougly 10° (e.g. Livio, 1989; Livio & Soker, 1988; Taam & Bodenheimer, 1989). With such a non-spherical distribution of circumstellar matter, and recalling that the inclination of RZ Eri is 89°, the above values are modified as follows: $M \sim 2 \cdot 10^{-7} M_\odot$ if $r \sim 60$ U.A. and $M \sim 2 \cdot 10^{-4} M_\odot$ if $r \sim 1800$ U.A.

These values for the total mass appear to be quite moderate. Thus, the mass loss process from RZ Eri B can be taken into account to explain the origin of the circumstellar matter surrounding the system.

6. The eclipsing system

Before analyzing the light curve of the eclipsing system, it is necessary to correct the photometric data for the variability of the secondary component. From the results of Sect. 4, we have chosen to use only the observations from the season 1987–1988 because, in this case only, the variability is well-described by our Fourier analysis, and it is possible to remove safely the effects of the spots, of the reflection and of the activity cycle.

Unfortunately, the nature of the spots is unknown, i.e. are they bright or dark ? Thus, the value of the magnitude of the secondary component without spots is unknown. For this reason, the analysis of the light curve has been made for both values of the corrected visual magnitude of the secondary : $< m > =$

Table 6. Parameters of RZ Eri from the analysis of the light curve with EBOP program. The primary radius is in unit of orbital semi-major axis a. The uncertainties are the internal errors from EBOP.

		A. V band	B. V band	C. B band
		< m >= 8.847 (mean)	< m >= 8.745 (maxi)	< m >= 9.262 (mean)
Primary radius	r_A	0.0385 ± 0.0006	0.0385 ± 0.0005	0.391 ± 0.0009
ratio of radii	k	2.44 ± 0.03	2.44 ± 0.03	2.43 ± 0.03
oblateness		0.00009 ± 0.00124	0.00009 ± 0.00124	0.00009 ± 0.00129
eccentricity	e	0.377± 0.008	0.377 ± 0.008	0.376 ± 0.008
long. of periastron	ω	−47°.3 ± 1°.2	−47°.3 ± 1°.2	−47°.0 ± 1°.2
inclination	i	89°.31 ± 0°.13	89°.30 ± 0°.13	89°.16 ± 0.10
ratio of central surf. bright.		0.109 ± 0.003	0.119 ± 0.003	0.051 ± 0.001
normalized prim. lum.	L_A	0.627	0.605	0.786
normalized sec. lum.	L_B	0.372	0.394	0.213
res. st. dev.	σ_{res}	$0^m.0047$	$0^m.0047$	$0^m.0037$

8.745 and 8.847, corresponding respectively to the maximum and to the mean luminosity of the starspot light curve (see Fig. 6a). The corrected magnitudes have been calculated as follows:

i) Outside eclipses

$$m^{corr}(t) = -2.5\log_{10}(E^{obs}(t) - E_B(t) + < E_B >) \quad (3)$$

where $< E_B > = \exp_{10}(-0.4 < m >)$, $E_B(t)$ is the "observed" value of the secondary flux derived from the fitted curve in Fig. 5 and $E^{obs}(t)$ is the flux of RZ Eri calculated from Table 1.

ii) Primary eclipses

Equation 3 is also valid, because the secondary component is completely visible during the whole primary eclipses.

iii) Secondary eclipses

$$m^{corr}(t) = -2.5\log_{10}(f(t) < E_B > + E_A) \quad (4)$$

where $E_A = \exp_{10}(-0.4 m_A)$ is the primary flux ($m_A = 8.269$ in the V band and 7.878 in the B band), $< E_B >$ is as above and $f(t) = (L_B - L_B^{ecl}(t))/L_B$. This factor, which varies from 1 (outside eclipses) to 0.788 (bottom of the secondary eclipses), has been evaluated from the results of a preliminary calculation on the raw data, i.e. without any correction for the secondary variability. The term L_B^{ecl} is the fraction of the secondary luminosity eclipsed.

The corrected light curve for the eclipsing system has been analysed by means of the EBOP program (Etzel, 1980). Three calculations have been made, two for the m_V data, for $< m > =$ 8.745 (maximum) and 8.847 (mean), and one for the m_B data, for $< m > = 9.262$ (mean). The values for the period and T_o are those of Sect. 2. The adopted limb darkening factors for the primary and secondary components are 0.58 and 0.72 for the V band, 0.80 and 0.95 for the B band, while the gravity darkening factors are respectively 0.92 and 0.45 for the V band, 1.13 and 0.57 for the B band (Binnendijk, 1974; Grygar et al., 1972; Martynov, 1973). Recent results indicate that for late type stars with convective atmospheres, the gravity darkening coefficient is about one third of the value of radiative atmosphere (Lucy, 1967; Nakamura & Kitamura, 1989). We used such low values for RZ Eri B. In any case, the choice of gravity darkening coefficients proves to have negligible effect on the derived elements of RZ Eri . The light curves having been corrected for the reflected light, the corresponding factors in the EBOP program have been put to zero. According to the estimation of the masses by Popper (1988), we have adopted a mass ratio of 0.96.

The result of our calculations with the EBOP program are given in Table 6 and Fig. 11 shows the calculated light curve in case B of Table 6. These results are very similar to those of Popper (1988), except for our uncertainties which are smaller by a factor of about 10. It is noteworthy that our residual standard deviations are very small. By adopting Popper's value *asini* = 72.5 ± 2.3$R_\odot$ (from his radial velocity curves) we derive:

$$R_A = 2.79 \pm 0.12 R_\odot$$
$$R_B = 6.80 \pm 0.23 R_\odot$$

By using in addition the radial velocity amplitudes $K_A = 48.9 \pm 1.3\,km\,s^{-1}$ and $K_B = 50.8 \pm 1.0\,km\,s^{-1}$, we obtain:

$$M_A = 1.69 \pm 0.06 M_\odot$$
$$M_B = 1.63 \pm 0.13 M_\odot$$

7. Rotational synchronisation and orbital circularization

In a circularized binary system (e = 0), the synchronous rotation of the components is defined by $P_{rot} = P_{orb}$. In a system with non-circular orbit, the equilibrium is reached for a value $P_{ps} < P_{orb}$, caused by the fact that tidal interaction is strongest around periastron (Hut, 1981; Hall, 1986). P_{ps} is the pseudosynchronous period, which is function of the orbital eccentricity only (see Eq.(42) in Hut (1981)). In the case of RZ Eri, the value e = 0.377 implies that $P_{ps} = 0.52 \cdot P_{orb} = 20^d.4$.

It was shown in Sect. 4 that the minimum period for the starspot variability of RZ Eri B was observed in 1984, with a value of $34^d.5$. Because of the differential rotation as a function of stellar latitude, this value is a superior limit of the equatorial rotation velocity and it may be supposed that P_{rot} is of the order or 34d at the equator. Thus, for RZ Eri B, P_{rot} is about 1.7 times larger than P_{ps}.

In the case of RZ Eri A, the rotational period is not well defined. According to Popper (1988), the lines of the hotter star in the spectrum of RZ Eri are appreciably broadened, the rotational velocity being estimated at $50\,km\,s^{-1}$. On the other hand, a value of $70\,km\,s^{-1}$ was obtained by Levato (1975). From the values of

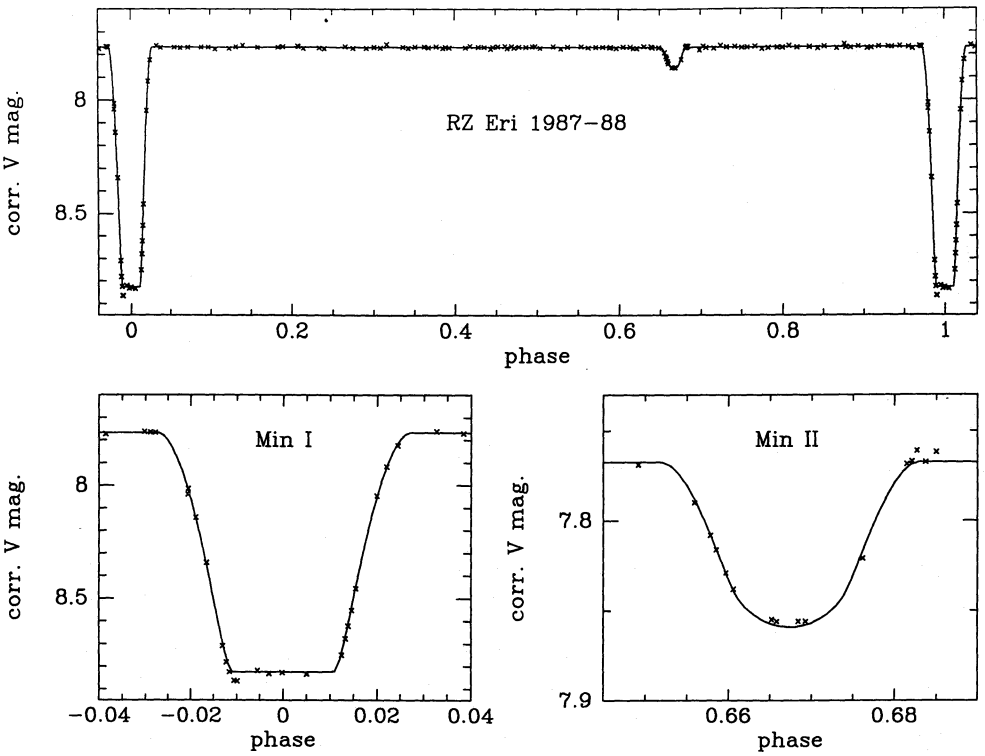

Fig. 11. Solution of the EBOP program, after correction of the data for the variability of RZ Eri B

Table 7. Parameters of the 4 systems in Fig. 12. The data on Capella and TZ For are by Andersen et al. (1991) and those on AI Phe by Andersen et al. (1988). The ages are derived from the evolutionary tracks by Maeder & Meynet (1988).

	Capella	TZ For	RZ Eri	AI Phe
Masses ($M_\odot$)				
hotter comp. A	2.5 ± 0.2	1.95 ± 0.03	1.69 ± 0.06	1.195 ± 0.004
cooler comp. B	2.6 ± 0.4	2.05 ± 0.06	1.63 ± 0.13	1.236 ± 0.005
P_{orb} (d)	104.02	75.67	39.28	24.59
eccentricity	0.	0.	0.377	0.189
P_{ps} (d)	104.02	75.67	21.4	20.2
P_{rot} A (d)	7.8 ± 0.9	4.7 ± 0.3	2.4 ± 0.5	23.1 ± 6.0
P_{rot} B (d)	80 ± 35	105 ± 28	34.5 ± 2	24.9 ± 4.5
a ($R_\odot$)	160.1	119.5	72.5	47.8
age (10^9y)	0.82	1.8	3.3	8.5

radius R_A and inclination i, it follows that $P_{rot} \cong 2.4 \pm 0^d.5$. This value is much smaller than P_{ps}.

Thus, *RZ Eri A and RZ Eri B rotate respectively faster and slower than the pseudosynchronous period.*

It was shown by Mayor & Mermilliod (1984) that, in a sample of binaries with similar components, all binaries with periods shorter than a cutoff period P_{cut} have circular orbits. In the case of main sequence spectroscopic binaries, P_{cut} varies with age, ~ 4 d in pre-main-sequence stars, $\sim 5^d.7$ in the Hyades and Praesepe, ~ 10 d in M67 and ~ 15 d in the halo; for red giants, P_{cut} is about 150 d (Mayor & Mermilliod, 1984, Latham et al., 1988; Jasniewicz & Mayor, 1988; Andersen et al., 1991).

According to Zahn (1977, 1989), binaries formed with stars having convective envelopes (this is the case of RZ Eri B) should synchronize much faster than they circularize. The circularization and synchronization times are proportional respectively to $(a/R)^8$ and $(a/R)^6$. Thus, because of the above results, it is not surprising that the orbit of RZ Eri is still not circularized (e = 0.377). In this context, the case of RZ Eri is especially interesting. It is fruitful to compare the evolutionary stages of its both components with those of three similar binaries studied by Andersen et al. (1988, 1991), AI Phoenicis, TZ Fornacis and Capella (α Aurigae). Some of the properties of the four systems are given in Table 7, and the position of these eight stars in the log L vs. log T_e diagram is shown in Fig. 12. The evolutionary tracks of Maeder & Meynet (1988) for stars of Pop I composition with initial masses of $1.20M_\odot$, $1.65M_\odot$, $2.00M_\odot$ and $2.55M_\odot$ are drawn. These models take into account the effects of overshooting and mass loss.

For $1.2M_\odot$ the track without overshooting of Maeder &

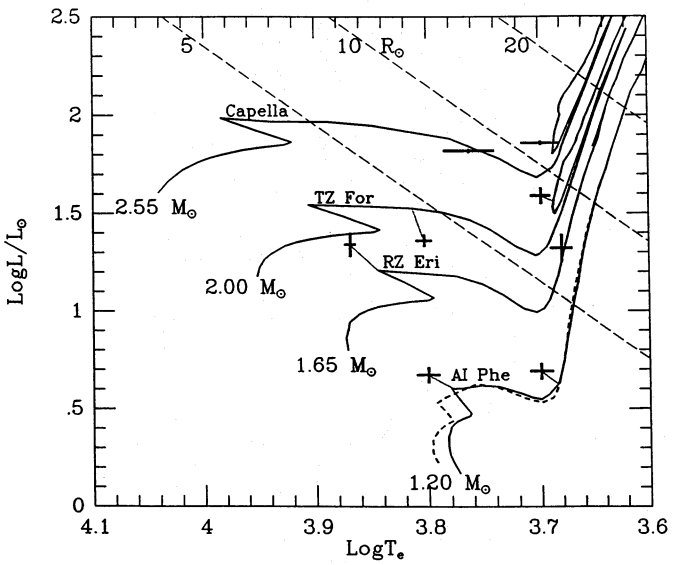

Fig. 12. Location of 4 binary stars in the $\log L/L_{\odot}$ vs. log Te diagram. The data for Capella, TZ For and AI Phe are by Andersen et al. (1988, 1991). The evolutionary tracks, with overshooting (continuous line) and without (dotted line), are by Maeder and Meynet (1988, 1991). The lines of constant radii are also noted

Meynet (1991) is also represented since these authors have noted that below a mass limit of about $1.6M_{\odot}$ there is no longer evidence of overshooting. Each of these tracks can be used to study one of the binaries, because the difference in mass between the components of the same system is small in the four cases; the correspondance between the tracks and the binaries is $2.55M_{\odot}$ for Capella, $2.00M_{\odot}$ for TZ For, $1.65M_{\odot}$ for RZ Eri and 1.20 for AI Phe.

Some discrepancies between the tracks and the location of the stars can be noted, in particular for TZ For A and AI Phe A and B. They can be due to:

i) difference in chemical composition between the stars and the Pop I tracks;
ii) unprecise values of log T_e and log L;
iii) effects of a mass exchange from the cooler to the hotter components.

In any case, these small discrepancies will not affect the results of the following discussion. From Table 7, the following remarks for the understanding of the circularization and synchronization mechanisms can be made:

A) Two systems have circularized their orbits: TZ For and Capella. As noted by Andersen et al. (1991), the cooler components in both systems Capella and TZ For appear to be in the core helium burning phase, i.e. at the base of the loop (the clump) in the red giant branch (RGB). This is the fundamental point in this discussion, because the radii of Capella B and TZ For B were larger in their past evolution, when these stars were at the first tip of the RGB. According to Andersen et al., the circularization of the orbits in these two systems occured mainly at this stage (first RGB tip) since the circularization times are proportional to $(a/R)^8$ (Zahn, 1977). Note that the same argument was used by Burki & Mayor (1983) to explain the circular orbits of the supergiant binaries in their blue loop evolution.

B) Two systems have not yet circularized their orbits: RZ Eri and AI Phe. The evolutionary tracks of Maeder & Meynet (1988) for the inital masses $1.7M_{\odot}$ and 1.20 are characterized by an absence of clump phase. Thus, *RZ Eri B and AI Phe B were never larger than yet in the past and these systems have not experienced phases of very efficient circularization* as it was the case for Capella and TZ For.

C) In the three systems RZ Eri, TZ For and Capella, the hotter component rotates much faster than the pseudosynchronization. For these components, the braking mechanisms were unable to pseudosynchronize the rotation during the evolution from the ZAMS.

D) The cooler component of RZ Eri rotates $\sim$ 1.7 times slower than the pseudosynchronization. The radius of RZ Eri B increased by a factor of about 2.5 during the last $40{\cdot}10^6$y, i.e. since the end of the main-sequence phase. This had consequences on the external rotation of the star. Indeed, during the evolution off the main sequence, the angular rotation of a star will decrease rapidly due to the increase of moment of inertia and to the action of magnetic braking (Habets & Zwaan, 1989). As a result of theses actions, the rotation of an evolving component in a binary system can become slower than the pseudosynchronous rotation. Gray & Endal (1982) showed that the *vsini* values of the K giants in the Hyades have decreased by a factor of about 40 with respect to their estimated values on the ZAMS. In conclusion, the slow rotational velocity of RZ Eri B can be simply explained in terms of recent evolutionary effects.

E) For the cooler components of TZ For and Capella, the ratio $P_{rot}/P_{ps} = 1.4 \pm 0.4$ and 0.8 ± 0.3 respectively. Thus it is possible to admit that these components are nearly synchronised. Because of the different evolutionary stages of TZ For B and Capella B, with respect to RZ Eri B (see points A) and B)), it is not excluded that the rotation of these two components were slower than presently before their ascention to the RGB tip and that the tidal processes have accelerated their rotation during the RGB phases.

F) Taking into account the uncertainties on P_{rot}, both components of AI Phe seem to be pseudosynchronized. This is an important difference with the case of RZ Eri (see points C) and D)). Indeed, the components of both systems are in similar evolutionary stages and both systems are not circularised, but neither the hotter (rotates faster) nor the cooler (rotates slower) components of RZ Eri are pseudosynchronized. A possible explanation for this difference is simply that the components are 1.5 times closer (see value of a) and 2.5 times older in AI Phe than in RZ Eri, so the required time for the pseudosynchronisation has been reached in AI Phe only. Finally, note that the evolutionary phases of the components of the four systems, as described here, are confirmed by the following remark. In a binary system, it is very unlikely to observe both components in a rapid evolutionary stage. Cap A and TZ For A being crossing the Hertzsprung gap, these are the cooler components which are most probably in a slow evolutionary stage (core helium burning). RZ Eri A and AI Phe A having not finished the main-sequence phase, it is thus not excluded that their cool companions are in a rapid evolutionary phase.

Conclusions

The main results obtained in this paper on RZ Eri are the following:

1. The existence of a secondary eclipse at phase 0.67 is confirmed.
2. The primary component, an A8-F0IV star, was stable during the 12 years of the survey.
3. The secondary component, a G8-K2IV-III star, exhibits 3 kinds of stellar variability:
   - A starspot effect with a period of about 35 d (stellar rotation), varying from year to year.
   - A reflection effect of the light from the primary component, with a period of $39^d.28254$ (the orbital period)
   - A long-term variability, tentatively attributed to a stellar activity cycle.
4. The solution of the light curve of the eclipsing system, made with the program EBOP, confirms the results of Popper (1988). In particular, $e = 0.377$ and $i = 89°.3$. By using in addition the solution of Popper for the radial velocity curves, it was found $R_A = 2.79 \pm 0.12 R_\odot$, $R_B = 6.80 \pm 0.23 R_\odot$, $M_A = 1.69 \pm 0.06 M_\odot$, $M_B = 1.63 \pm 0.13 M_\odot$ for the radii and masses of the primary and secondary components.
5. The multicolour photometric analysis of the two components reveals a high value for the reddening, E(B-V) = 0.20. Because of the distance, 180pc, and galactic latitude, −33°, it is probable that the major part of this reddening is circumstellar rather than interstellar.
6. The spectral types of both components and the amount of reddening are confirmed by the analysis of the UV spectra of RZ Eri taken by the IUE satellite.
7. The presence of circumstellar matter around RZ Eri is confirmed by the detection of an IR excess (Busso et al., 1990). This matter has probably been expelled from RZ Eri B during stellar evolution by normal mass loss processes.
8. The orbit is not yet circularized. By comparing the evolutionary status of RZ Eri with those of Capella and TZ For recently studied by Andersen et al. (1991), one can propose the following scenario: the binary systems with periods larger than at most 39 d and with components of masses in the range $1.7 M_\odot$ to $2.5 M_\odot$ will not have their orbit circularized before the first evolving star has passed through the first tip of the RGB phase. Of course, the values given here for the period limit and for the mass range are only indicative, since they are based on these few systems.
9. For RZ Eri, the pseudosynchronous period of rotation is $P_{ps} = 0.52\ P_{orb} = 20^d.4$. Thus, the hotter and cooler components rotate respectively faster ($P_{rot} \cong 2^d.5$) and slower ($P_{rot} \cong 34$ d) than P_{ps}. Our explanation is:
   - **i)** The hotter component has not yet left the main-sequence and the braking mechanisms (tidal and magnetic effects, radius expansion) had not enough time to achieve the synchronization.
   - **ii)** The rotation of the cooler component decreased rapidly during its recent crossing of the Hertzsprung gap because of the radius expansion.

Appendix A: Classification of the two components of RZ Eri

From Tables 2 and 3, it is possible to calculate the various colour indices and parameters useful for a photometric study of both components of RZ Eri.

A.1. Reddening

The photometric box method (Golay et al. 1969; Nicolet 1981a) was applied to the Geneva colours of both the primary and secondary components. In the Geneva photometric catalogue (Rufener, 1988) 4 stars were found with the following properties:

- **i)** they have the same colours as the primary or the secondary components;
- **ii)** they belong to an open cluster of known distance and reddening;
- **iii)** they have an estimate of their spectral type in the litterature, although sometimes approximative.

Table 8. List of the twin stars of the components of RZ Eri, according to the photometric box method.

Cluster	star number	sp-type	$E(B_2\text{-}V_1)$	reference for $E(B_2\text{-}V_1)$
primary				
NGC 7243	483	(A6)	0.19	Nicolet, 1981b
secondary				
NGC 6633	101	G8II	0.18	Nicolet, 1981b
IC 4756	38	(K0)	0.17	Smith, 1983; Schmidt, 1978
IC 4756	44	(K)	0.17	Smith, 1983; Schmidt, 1978

Table 8 presents the characteristics of these stars, which can be considered as twin stars of the components of RZ Eri, according to the properties of the photometric box method. It is especially noteworthy that the colour excesses $E(B_2\text{-}V_1)$ of the 3 clusters in Table 8 are very similar. A mean value

$$E(B_2 - V_1) = 0.18$$

can be adopted, corresponding to a value E(B-V) = 0.20 in the Johnson UBV system. This value of the reddening can be adopted for the two components of RZ Eri.

A.2. Spectral types

From the values of $(B_2\text{-}V_1)$ and of the Geneva photometric parameter d (see Golay (1980) for the definition of d) for both components, by using the calibrations spectral types vs. colour indices of Meylan et al. (1980) and by adopting the above value for the reddening, we deduce the most probable spectral types:

Primary	A8-F0IV
Secondary	G8-K2IV-III

According to Popper (1988), there was a discrepancy between the colours and spectral types of both components. The analysis of Popper is the following: i) the reddening is negligible; ii) the spectral types estimated from (B-V) values are F5 for the primary components and K2 III or K5 V for the secondary components; iii) the primary and secondary components are respectively redder and bluer in the index (U-B) than normal stars having the same values of (B-V). These discrepancies disappear if our value

of the reddening $E(B_2\text{-}V_1) = 0.18$ is adopted. This is immediately apparent by plotting the position of both components in a $[U\text{-}B_2]$ vs. $[B_2\text{-}V_1]$ diagam (colours from Tables 2 and 3, standard sequences and reddening lines from Fig. 2 and 3 in Golay (1980) or Fig. 12 in Crawford & Mandwewala (1976)): the position of the dereddened components are near the sequences of luminosity classes IV or III. Indeed, the use of such a two–colour diagram confirms that both components of RZ Eri are reddened, by roughly the same amount of circumstellar and interstellar material.

Note that these luminosity classes are in agreement with the gravity determinations of Popper (1988) : $\log g = 3.75$ for the primary and 2.97 for the secondary. On the other hand, the photometric calibration of Kobi & North (1990) gives a similar value for the gravity of the primary: 3.7 ± 0.1.

A.3. Effective temperatures

The intrinsic colour indices $[B_2\text{-}V_1]_0$ are 0.052 for the primary and 0.640 for the secondary components. These values correspond to intrinsic UBV indices $(B\text{-}V)_o$ of 0.244 and 0.961 from the calibrations of Meylan & Hauck (1981). The T_e value for the primary can be estimated to 7390 ± 100 K from Popper (1980) by using $(B\text{-}V)_0$ and this value is in very good agreement with T_e obtained by using the calibration by Kobi and North (1990). For the secondary component, the calibration of Popper (1980) cannot be used since it gives too low temperatures for late-type giants (Andersen et al., 1991). The study of Bell and Gustafsson (1989) allows a T_e estimation of 4820 ± 100K for a K0III-IV star, in very good agreement with the value $T_e = 4790$ K obtained for a K0III star by using the calibration of Ridgway et al. (1980). So we adopt:

$\log T_e = 3.869 \pm 0.005$ for the primary
$\log T_e = 3.68 \pm 0.01$ for the secondary

A.4. Luminosities

From the values of T_e and of the radii (Sect. 6), the following values are determined:

For the primary	$\log L/L_\odot$	1.34 ± 0.06
	M_{bol}	1.40 ± 0.15
	M_V	1.41 ± 0.15
For the secondary	$\log L/L_\odot$	1.32 ± 0.07
	M_{bol}	1.45 ± 0.17
	M_V	1.85 ± 0.17

where the bolometric corrections from Popper (1980) have been used. The difference in M_V between the two components, 0.44, is in moderately good agreement with the difference in apparent visual magnitudes, 0.59 (see Tables 2 and 3).

Another estimation of the visual absolute magnitudes can be obtained by using the relation :

$$M_V = -5 \log R - 10 F_V + 42.255$$

where the visual surface flux can be obtained via F_V vs. $(B\text{-}V)_0$ relation (Popper, 1980). The values $M_V = 1.34$ and 1.91 are obtained for the primary and secondary components, being in good agreement with the above determinations.

From the apparent and absolute magnitudes and by using $A_V/E(B_2\text{-}V_1) = 3.58$ (Crawford and Mandwewala, 1976) a distance of 180 pc is derived for RZ Eri.

A.5. Age

On the basis of the radii and masses derived in section 6, an estimation of the age of the system can be obtained. By using the revised version of the evolutionary tracks by Maeder and Meynet (1988), for an initial mass of $1.65 M_\odot$ and a chemical composition (X,Z)=(0.70,0.02) (see section 7 and Figure 12), an evolutionary age of $\log t = 9.32$ is estimated.

Acknowledgements. We warmly thank our colleagues F. Rufener, N. Cramer and C. Richard for the photometric reduction of these measures of RZ Eridani, M. Burnet for the technical maintenance of the Geneva station at La Silla during the whole survey, B. Nicolet for the calculations with the photometric box method, G. Meynet for the calculation of evolutionary tracks, C. Waelkens (Katholieke Instituut, Leuven) for helpful discussions and the referee, Dr. A. Gimenéz, for his comments and suggestions. One of us (Z. Kvíz) appreciated particularly given advice by P. B. Etzel concerning use of EBOP code. This work was partially supported by the Swiss National Science Foundation.

References

Andersen, J., Clausen, J.V., Gustafsson, B., Nordström, B., VandenBerg, D.A. 1988, A&A **196**, 128
Andersen, J., Clausen, J.V., Nordström, B., Tomkin, J., Mayor, M. 1991, A&A , in press
Bell, R.A., Gustafsson, B. 1989, MNRAS **236**, 653
Bohlin, R.C., Savage, B.D., Drake, J.F. 1978, ApJ **224**, 132
Binnendijk, L, 1974, Vistas in Astronomy **16**, 61
Burki, G. 1991, The High Precision Photometry in the Study of Variable Stars, in Precision Photometry: Astrophysics of the Galaxy, Ed. A.G. Davis Philip, Davis Press, Schenectady, p. 183
Burki, G., Mayor, M. 1983, A&A **124**, 256
Burnet, M., Rufener, F. 1979, A&A **74**, 54
Busso, M., Scaltriti, F., Ferrari-Toniolo, M., Origlia, L., Persi, P., Robberto, M. Silvestro, G 1990, Mem. Soc. astr. ital. **61**, 77
Caton, D.B. 1986, AJ **91**, 132
Cesco, C.U., Sahade, J. 1945, ApJ **101**, 370
Cramer, N. 1982, A&A **112**, 330
Cramer, N., Maeder, A. 1979, A&A **78**, 305
Crawford, D.L., Mandwewala, N. 1976, PASP **88**, 917
Dobias, J.J., Plavec, M.J. 1989, Space Sci. Rev. **50**, 340
Etzel, P.B. 1980, EBOP user's guide, 3rd edition, UCLA Astron. Astrophys.
Feckel, F.C., Moffet, T.J., Henry, G.W. ApJS **60**, 551
Glebocki, R., Sikorski, J., Bielicz, E., Krogulec, M. 1986, A&A **158**, 392
Golay, M., Peytremann, E., Maeder, A. 1969, Publ. Obs. Genève, Série A, **76**, 44
Golay, M. 1980, Vistas in Astronomy **24**, 141
Gray, D.F., Endal, A.S. 1982, ApJ **254**, 162
Grygar, J., Cooper, M.L., Jurkevich, I. 1972, Bull. Astron. Inst. Czechoslovakia **23**, 147
Habets, G.M.H.J., Zwaan, C. 1989, A&A **211**, 56
Hall, D.S. 1976, in Multiple Periodic Variable Stars, IAU coll. 29, ed. W.S Fitch, Budapest, p. 287
Hall, D.S. 1986, ApJ **309**, L83
Hall, D.S, Kreiner, J.M. 1980, Acta astr. **30**, 387
Heck, A., Egret, D., Jaschek, M., Jaschek, C. 1984, ESA SP-1052, IUE Low-Dispersion Spectra Reference Atlas - Part I. Normal Stars.

Hut, P. 1981, A&A **99**, 126
Imbert, M. 1991, private communication
de Jager, C., Niewenhuijzen, H., van der Hucht, K.A. 1988, A&AS **72**, 259
Jasniewicz, G., Mayor, M. 1988, A&A **203**, 329
Kobi, D., North, P. 1990, A&AS **85**, 999
Kvíz, Z. 1989, Space Sci. Rev. **50**, 351
Latham, D.W., Mazeh, T., Carney, B.W., Mc Crosky, R.E., Stefanik, R.P., Davis, R.J. 1988, in Calibration of Stellar Ages, Eds. A. Upgren, A.G.D. Philip, L. Davis Press, Schenectady, p. 185
Levato, H. 1975, A&AS **19**, 91
Livio, M. 1989, Space Sci. Rev. **50**, 299
Livio, M., Soker, N. 1988, ApJ **329**, 764
Lucy, L.B. 1967, Zeitsch. für Astrophys. **65**, 89
Lucke, P.B. 1978, A&A **64**, 367
Maeder, A., Meynet, G. 1988, A&AS **76**, 411
Maeder, A., Meynet, G. 1991, A&AS, **89**, 451
Martin, P.G. 1978 in Cosmic Dust, Clarenlon Press, Oxford, p. 40
Martynov, D.Ya. 1973, Eclipsing systems with deformed components, in Eclipsing Variable Stars, Ed. V.P. Tsesevich, Holsted Press Book, John Wiley and Sons, New York, p. 128
Mayor, M., Mermilliod, J.C. 1984, in Observational Tests of the Stellar Evolution Theory, IAU Symp. 105, Eds. A. Maeder, A. Renzini, Reidel Publ., Dordrecht, p. 411
Meylan, G., Python, M., Hauck, B. 1980, A&A **90**, 83
Meylan, G., Hauck, B. 1981, A&AS **46**, 281
Montesinos, B., Giménez, A., Fernández-Figueroa, M.J. 1988, MNRAS **232**, 361
Murray, J., Driessen, C., Talavera, A. 1990, in Evolution in Astrophysics, ESA-SP 310, ed. E.J. Rolfe. p. 609
Nakamura, Y., Kitamura, M. 1989, Space Sci. Rev. **50**, 353
Nicolet, B. 1981a, A&A **97**, 85
Nicolet, B. 1981b, A&A **104**, 185
Popper, D.M. 1980, ARA&A **18**, 115
Popper, D.M. 1988,AJ **96**, 1040
Popper, D.M., Ulrich, R.K., 1977, ApJ **212**, L131
Ridgway, S.T., Joyce, R.R., White, N.M., Wing, R.F. 1980, AJ **235**, 126
Rodono, M. 1986, Starspots and Plages, in Highlights of Astronomy, Ed. J.P. Swings, p. 429
Rucinski, S.M. 1969, Acta astr. **12**, 245
Rufener, F. 1964, Publ. Obs. Genève, Série A, n^o 66
Rufener, F. 1985, Approaches to Photometric Calibrations, in Calibrations of Fundamental Stellar Quantitites, IAU symp. 111, Eds. D.S. Hayes, L.E. Pasinetti, A.G. Davis Philip, Reidel Publ., Dordrecht, p. 253
Rufener, F. 1988, Catalogue of Stars Measured in the Geneva Observatory Photometric System, 4^e Edition, Obs. Genève
Rufener, F., Nicolet, B. 1988, A&A **206**, 357
Sarma, M.B.K. 1986, in Highlights of Astronomy, ed. J.P. Swings, p. 443
Scaltriti, F., Busso, M. et al. 1984, A&A **139**, 25
Schmidt, E.G. 1978, PASP **90**, 157
Seaton, M.J. 1979, MNRAS **187**, 73
Söderhjelm, S. 1980, A&A **89**, 100
Smith, G.H. 1983, PASP **95**, 296
Strassmeier, K.G., Hall, D.S., Boyd, L.J., Genet, R.M. 1989, ApJS **69**, 141
Wood, D.B. 1971, AJ **76**, 701
Wood, D.B. 1972, A computer program for modeling non–spherical eclipsing binary star systems, Publ. of the Goddard Space Flight Center X–110–72–473
Taam, R.E., Bodenheimer, P. 1989, ApJ **337**, 849
Wu, C.C., Ake, T.B., Bogess, A., Bohlin, R.C., Imhoff, C.L., Holm, A.V., Levay, Z.G., Panek, R.J., Schiffer, F.H., Turnrose, B.E. 1983, IUE NASA Newsletter N^o 22
Zahn, J.P. 1977, A&A **57**, 383
Zahn, J.P. 1989, A&A **220**, 112

This article was processed by the author using Springer-Verlag LaTeX A&A style file 1990.